Virtual Network Embedding with Adaptive Modulation in Flexi-grid Networks

Lin, Rongping; Luo, Shan; Zhou, Jingwei; Wang, Sheng; Cai, Anliang; Zhong, Wen-De; Zukerman, Moshe

Published in:
Journal of Lightwave Technology

Published: 01/09/2018

Document Version:
Post-print, also known as Accepted Author Manuscript, Peer-reviewed or Author Final version

License:
Unspecified

Publication record in CityU Scholars:
Go to record

Published version (DOI):
10.1109/JLT.2017.2764940

Publication details:
Lin, R., Luo, S., Zhou, J., Wang, S., Cai, A., Zhong, W-D., & Zukerman, M. (2018). Virtual Network Embedding with Adaptive Modulation in Flexi-grid Networks. *Journal of Lightwave Technology*, *36*(17), 3551-3563. https://doi.org/10.1109/JLT.2017.2764940

Virtual Network Embedding with Adaptive Modulation in Flexi-grid Networks

Rongping Lin, Shan Luo, Jingwei Zhou, Sheng Wang, *Member*, *IEEE*, Anliang Cai, Wen-De Zhong, *Senior Member*, *IEEE*, and Moshe Zukerman, *Fellow*, *IEEE*

***Abstract*—Network virtualization has been proposed as a promising method to mitigate the ossification of the Internet by allowing multiple heterogeneous virtual networks (VNs) to coexist on a shared substrate network. One of the major challenges in this method is the VN embedding (VNE) problem of how to map efficiently the virtual nodes and links onto the substrate network considering constraints associated with different substrate networks. This paper aims to solve the VNE problem with geographical constraints in the context of flexi-grid optical networks where modulation modes can be selected optimally. We provide an integer linear programming (ILP) formulation for the problem with the objective function of minimizing the embedding cost of an arriving VN. To achieve scalability, we also propose three polynomial-time heuristic algorithms where virtual links are embedded sequentially by three different sequences, respectively. We find that the sequence considering the bandwidth requirements of the virtual links outperforms the others. Such a sequence leads to a cost-effective VNE solution in terms of spectrum resource usage, which aims to optimize modulation modes and transmission distances of the virtual links that have high bandwidth requirements. Numerical results show that the heuristic algorithm with the sequence considering the bandwidth requirements performs closely to the ILP for a small size network, and we also demonstrate its applicability to larger networks.**

***Index Terms*—Virtual network embedding, flexi-grid optical network, modulation mode, integer linear programming.**

I. Introduction

Cisco 2015 White Paper [1] states that the global IP traffic will reach 2.3 Zettabytes by the end of 2020. This represents a significant challenge for the future Internet, particularly, considering the explosive growth of user demand, the accelerated development of cloud computing and the diversification of network applications and services. Facing these challenges, there is a need to improve the flexibility of the costly and scarce Internet resources. To this end, the network virtualization technology has been proposed and it is now considered an important feature of the next generation Internet architecture.

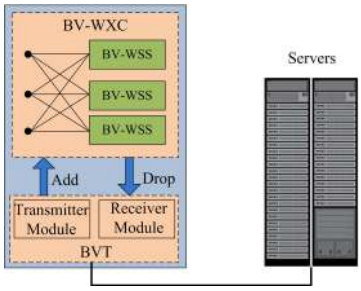

Fig. 1. Physical node in flexi-grid networks.

In a virtualized network, the infrastructure provider (InP) manages the substrate network that consists of physical links and physical nodes. Physical links are optical fibers that provide connections between physical nodes. An example of physical node is shown in Fig. 1, both network component and servers are introduced. The network component includes bandwidth variable transponder (BVT) and bandwidth variable wavelength cross connect (BV-WXC) that has multiple bandwidth variable wavelength selective switches (BV-WSSs) installed. The network component is used to provide optical channels for end-to-end connections. Servers that provide computation resources, i.e. CPU resources, are directly connected to the BVT. The network function virtualization (NFV) can also be implemented based on this system, where NFV technology enables integrated network devices to be implemented as software running on general-purpose servers for cost saving and flexible management purposes [2], [3].

With bandwidth resources and computation resources provided by InP, the service provider (SP) creates virtual networks (VNs) and offers services to users [4], where a VN consists of virtual nodes and virtual links. Virtual nodes are the nodes that have computation requirements and the virtual links represent the end-to-end connections with bandwidth requirements between virtual nodes. Finding the optimal way to map a VN onto a substrate network under a given set of constraints is known as the VN embedding (VNE) problem. According to [5], the VNE problem can be decoupled into two phases: the virtual node embedding phase where the virtual nodes are mapped to the physical nodes under the constraints of physical nodes, which can be computation resource limitation or geographical constraint, and the virtual link embedding phase where the virtual links are mapped to physical paths

This work was supported by grants from the National Natural Science Foundation of China (NSFC) (61401070, 61303250, 61671130, 61701079), the Fundamental Research Funds for the Central Universities (ZYGX2014J002), the National Basic Research Program (China's 973 Program) (2013CB329103) and by a grant from the Research Grants Council of the Hong Kong Special Administrative Region, China [CityU 11216214].

R. Lin, J. Zhou and S. Wang are with the School of Communication and Information Engineering, University of Electronic Science and Technology of China (UESTC), China (e-mail: linrp@uestc.edu.cn, cleff.zhoujw@gmail.com, wsh_keylab@uestc.edu.cn).

S. Luo is with the School of Astronautics and Aeronautic, UESTC, China (e-mail: luoshan@uestc.edu.cn).

W. D. Zhong is with the School of Electrical and Electronic Engineering, Nanyang Technological University, Singapore (e-mail: ewdzhong@ntu.edu.sg).

A. Cai and M. Zukerman are with the Department of Electronic Engineering, City University of Hong Kong, Hong Kong SAR (e-mail: anliancai2-c@my.cityu.edu.hk, m.zu@cityu.edu.hk).

under the bandwidth resource constraint. Specifically, if a virtual node is embedded to a physical node, a server is used to provide computation resources for the virtual node, and BV-WXC and BVT of the physical node are used for the optical channels that sustain the virtual links incident to the virtual node. However, if a physical node is traversed by an optical channel as an intermediate node, only BV-WXC is used for optical switching.

An example is shown in Fig. 2, where multiple VNs are embedded in a substrate network. The virtual nodes are mapped to physical nodes where computation resources are reserved, and the virtual links are mapped to physical paths where bandwidth resources are reserved. It is clear that a physical node or a physical link can be shared by different VNs. For simplicity, we only show virtual links e_1 and e_2 of two different VNs that are embedded into p_1 and p_2, respectively, where a physical node and a physical link are shared.

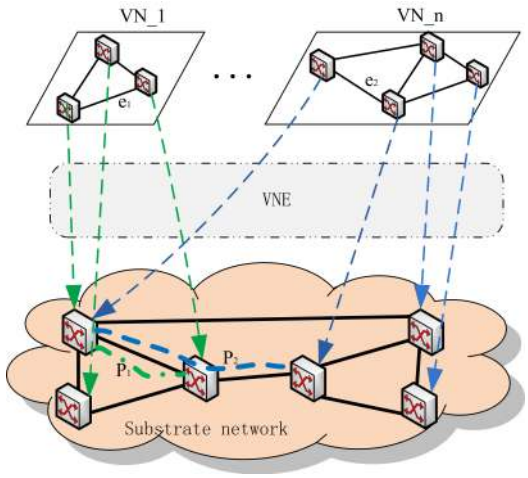

Fig. 2. VNE in network virtualization.

Meanwhile, facing an exponential increase of bandwidth demand, network operators rely on the high bandwidth of optical fiber and optical transmission and networking technologies to scale their networks to meet the demands. Traditional wavelength-division multiplexing (WDM) networks rely on fixed subcarrier frequencies (fixed grid) and allocate bandwidths with a fixed wavelength granularity. Setting up VNs over a WDM network therefore leads to underutilized wavelengths because normally capacity required by end-to-end connections will not be exactly equal to an integer multiple of wavelength capacity.

Compared to the WDM technology, the flexi-grid technology is of higher bandwidth utilization and provides better flexibility in spectrum allocation, and thus has been considered as a future optical transmission technology [6]. Nyquist WDM (NWDM) and optical orthogonal frequency-division multiplexing (OOFDM) are two approaches that motivate the model of the flexi-grid network. NWDM spectrally shapes carriers so that they potentially occupy a bandwidth close or equal to the Nyquist limit to tightly control the spectral extent of each wavelength channel [7]. NWDM has already been used in practice. For example, commercial coherent receivers use pulse-shaping which is based on the NWDM concept [8]. By comparison, OOFDM allows the spectrum of adjacent subcarriers to overlap and the subcarriers are spaced at the symbol rate [9], [10]. Although OOFDM has been extensively studied, to the best our knowledge, it has not reached the market yet. Anyway, both NWDM and OOFDM are considered under the umbrella of the flexi-grid network.

In flexi-grid optical networks, spectrum are allocated according to the bandwidth requirement of connection requests, where the just-enough spectrum resources are allocated at finer sub-wavelength granularities, e.g., a few GHz, than WDM. Moreover, the modulation mode used by subcarriers can further affect the spectrum efficiency, where short transmission distances with high order modulation usages can improve the spectrum efficiency, while long transmissions should apply low order modulations to keep the optical signal quality at acceptable levels. Usually, a transponder has constraints that limit transmission rate and modulation format selection, e.g., the baud-rate limitation of a transponder allows limited transmission rates with a low-order modulation format. In our paper, we assume that any admitted connection requires rate lower than the capacity of the transponder.

To the best of our knowledge, there was no published work on the VNE problem considering modulation selections in flexi-grid networks. This paper considers the VNE problem over flexi-grid optical networks, where modulation modes are adaptively selected to maximize the spectrum efficiency.

A. Related Work

There are two fundamentally different approaches to address the VNE problem. They are categorized as static and dynamic. For both categories, a substrate network is given. In static cases, all requests for VN set up, henceforth called *VN requests*, are known a priori, the VNE problem is a dimensioning problem to minimize resource usage under the condition that all the VN requests are satisfied. In dynamic cases, the VN requests arrive one-by-one and leave the substrate network after receiving services (connections takedown). The VNE problem is how to optimally allocate network resources for each arriving request. As the network resources are time variable, this case is more difficult and practical than the former case.

The authors of [11]–[13] focused on the static traffic scenarios, and considered also computation resource requirements at virtual nodes and bandwidth demands of virtual links. However, these VNE algorithms are limited to static scenarios and their dimensioning solutions may not be optimal for realistic scenarios with dynamic traffic where VN requests arrive over time and their demands of resources are not known in advance.

The authors of [14], [15] provided VNE algorithms applicable to dynamic scenarios, but without considering optical layer technologies such as WDM or flexi-grid. The VNE algorithms of [14], [15] allocate network resources for an arriving VN request based on the current network state. After the service, the VN request is terminated and cleared from the network. Then the network resources that were allocated to this VN

request are released for the requests arriving thereafter. These publications have considered limitations on node computation resources and also constraints associated with flow conservation and link bandwidth limitations. However, their models by their nature did not consider the constraints related to flexi-grid optical networks. In flexi-grid optical networks, the bandwidth resource is allocated in term of spectrum slots and modulation mode, i.e. the number of spectrum slots and the specific modulation mode determine the bandwidth and also the maximal distance that the optical signal can reach. At the same time, continuity and contiguity constraints must be satisfied, i.e., the same spectrum slots should be utilized along the lightpath (continuity), and the allocated spectrum slots in a link should be contiguous (contiguity).

The authors of [16] considered the dynamic scenario with the objective of maximizing revenues. They proposed an auxiliary graph with meta-nodes (clustering nodes), where virtual link mapping becomes the commodity flow problem among meta-nodes. In [17], [18], the VNE problem over flexi-grid optical networks was also investigated under the dynamic scenario aiming to minimize usage of spectrum slots. An auxiliary graph was constructed based on the available spectrum slots, and virtual node and link mappings were carried out on the auxiliary graph. To improve the performance of virtual link mapping, the number of spectrum slots of physical links is taken into consideration in virtual node mapping, where the physical nodes connecting the links that have more spectrum slots have a higher probability to find feasible lightpaths for the virtual links.

All existing publications on the VNE problem in flexi-grid networks ignore the effect of adaptively selecting modulation modes, and assume that the required number of spectrum slots is given. Considerable reduction of spectrum resources usage can be achieved when taking into consideration the optimal selection of modulation mode. In this paper, the VNE problem is investigated for flexi-grid optical networks with the aim to optimize the selection of modulation mode.

Other related publications that do not consider the VNE problem include the work described in [19]–[21]. The authors investigated problems of routing, modulation selection and spectrum assignment for end-to-end connections in flexi-grid optical networks, where the transmission distance of optical signal were taken into consideration and the choices of modulation modes were investigated to reduce spectrum resource usages. The work in [22] provided multicast protection in flexi-grid optical networks considering also the adaptive selections of modulation modes.

B. Organization

The remainder of this paper is organized as follows. Section II gives the preliminaries including the problem statement and definitions of virtual node and virtual link embeddings. Section III describes the ILP model of VNE in flexi-grid optical networks. In Section IV, we propose three heuristic algorithms for large networks. Section V evaluates both ILP and heuristic algorithms by simulations. Section VI concludes this paper.

II. Preliminaries

A. Problem Statement

The VNE problem in flexi-grid optical networks with dynamic VN requests can be stated as follows.

Given:

1) A substrate topology $G^s(N^s, L^s)$ is a directed graph representing the substrate network, where N^s is the set of physical nodes and L^s is the set of physical links. Physical nodes and links are given with their available computation resources and spectrum resources, respectively.
2) All the fibers in the network are assumed to be identical and each fiber carries F spectrum slots. Various modulation modes can be selected to maximize the efficiency of transmission.
3) We assume that if two nodes are connected by a physical link on one direction, they are also connected by another link in the opposite direction.
4) There are no wavelength converters in the network, which means a lightpath traversing multiple links must use the same spectrum slots.
5) An arriving VN request $G^v(N^v, L^v)$ is modeled as a directed graph, where N^v is the set of virtual nodes and L^v is the set of virtual links. The geographical constraint ensures that virtual node i is embedded to one of the physical nodes in $X(i)$, where $i \in N^v$.

Our goal is to embed the arriving VN request at a minimal cost. If the existing network cannot accommodate the request due to the lack of resources, this request will be blocked. Otherwise, we provide:

1) *Virtual node embedding information*: Each virtual node is mapped to a specific physical node and required computation resources are reserved at the physical node for the virtual node.
2) *Virtual link embedding information*: Each virtual link is mapped to a set of physical links in a cascade way that forms a lightpath connecting two physical nodes hosting the two virtual nodes of the virtual link, a proper modulation mode is selected, and spectrum slots along the lightpath are reserved accordingly.

B. Virtual Node and Virtual Link Embeddings

In general, approaches of heuristic solutions to the VNE problem, have been based on two phases: (1) virtual node embedding and (2) virtual link embedding considering bandwidth limitation. Here, because we consider flexi-grid networks, in our virtual link embedding phase, we must take into consideration also other substrate network constraints including continuity and contiguity. As in previous approaches, also in our study of flexi-grid networks, a VN request is successfully embedded into the substrate network if both virtual node and virtual link embedding phases are successful. Otherwise the embedding of the VN request fails.

In virtual node embedding, physical nodes are selected to serve virtual nodes and these physical nodes must have enough computation resources.

$$M_N(i) = t; \quad i \in N^v, t \in X(i), X(i) \subseteq N^s \tag{1}$$

Equation (1) implies that the virtual node i is embedded at the physical node t. With computation resource limitations, $p_i \leq U_t$ should be satisfied, where p_i and U_t are the required computation resource of virtual node i and the available computation resource of physical node t, respectively. With the geographical constraint of virtual node i, the physical node t should be in physical node set $X(i)$, to which the virtual node can be embedded.

In virtual link embedding, a physical path is set up to serve a virtual link which must meet the constraints of continuity and contiguity as follows.

$$M_L(e) = P_{M_N(d(e))}^{M_N(s(e))}; \quad e \in L^v \tag{2}$$

Equation (2) implies that the virtual link e is embedded in the physical path $P_{M_N(d(e))}^{M_N(s(e))}$, where $s(e), d(e), M_N(s(e))$ and $M_N(d(e))$ denote the source node of e, the destination node of e, the physical node where $s(e)$ is embedded and the physical node where $d(e)$ is embedded, respectively. Suppose $P_{M_N(d(e))}^{M_N(s(e))} = \{L_1, L_2, .., L_n\}$, where L_1 to L_n are physical links and are cascaded to be the path. $M_N(s(e))$ is the start node of L_1, and $M_N(d(e))$ is the end node of L_n. According to the contiguity constraint, the spectrum slots allocated at any link of $\{L_1, L_2, .., L_n\}$ are contiguous, which forms a spectrum band, and the spectrum bands allocated on all the physical links of $\{L_1, L_2, .., L_n\}$ are the same for this request, which forms an end-to-end optical channel. In addition, the modulation mode is properly selected according to the transmission distance. For example, we assume that the bandwidth of one spectrum slot is 12.5 GHz which can carry 12.5 Gb/s signal if the modulation mode is BPSK and carry 25 Gb/s signal if the modulation mode is QPSK. According to [19], [23], we assume the transmission ranges of BPSK, QPSK, 8QAM, 16QAM, 64QAM and 256QAM are 3000 km, 1500 km, 750 km, 375 km, 94 km, and 24 km, respectively. The spectrum usage varies if different modulation modes are used while obtaining the same bandwidth. Meanwhile, a frequency guard band between two adjacent optical channels is required to resolve the roll-off problem of optical filters [24], [25]. The following equation representing the relationship between bandwidth requirement and the number of spectrum slot usage is applied in this paper, where p is the bandwidth requirement in terms of the number of spectrum slots for conciseness, G is the frequency guard band in term of spectrum slots, and g is the actual number of slots needed when modulation mode mod is used in transmission, where $mod = 1, 2, 3, 4, 6, 8$ are for modulation efficiencies of BPSK, QPSK, 8QAM, 16QAM, 64QAM, 256QAM respectively [19].

$$g = \left\lceil \frac{p}{mod} \right\rceil + G \tag{3}$$

A virtual node is hosted on a physical node which is a source or destination of lightpaths in the substrate network, that provide connections for virtual links, and virtual node embedding and virtual link embedding are dependent on each other.

III. ILP Based Resource Allocation

Although ILP is formulated to solve a static (deterministic) optimization problem, our ILP based method applies to a practical dynamic set-up. When a VN request arrives, the ILP formulation is used for the current network resources to derive an embedding solution for the request. After its service is complete, the VN request leaves the network. The available network resources are dynamically changed according to request arrivals and departures. If a VN request cannot be accommodated because of lack of resources, the ILP cannot find a feasible solution as each VN request is forced to be accommodated by the ILP constraints. In the following, we provide in detail, the formulation of our ILP problem used for resource allocation.

Given:

$G^s(N^s, L^s)$: the substrate network, where N^s is the set of physical nodes and L^s is the set of physical links.

$G^v(N^v, L^v)$: the arriving VN request, where N^v is the set of virtual nodes and L^v is the set of virtual links.

$X(i)$: the set of physical nodes that virtual node i can be embedded, $X(i) \subseteq N^s$, $i \in N^v$. In this paper, the $X(i)$ is randomly generated similarly to [16].

c_k: computation unit cost at physical node k, $k \in N^s$.

c_{mn}: unit cost of a spectrum slot in physical link (m, n), $(m, n) \in L^s$. It is usually proportional to the length of the physical link.

p_i: the computation resource requirement of virtual node i, $i \in N^v$.

p_{ij}: the bandwidth requirement of virtual link (i, j), $(i, j) \in L^v$.

F: the maximal spectrum slot index of physical links in the network.

U_k: the number of residual computation resources at node k, $k \in N^s$, e.g. the number of available CPU resources can be provided at node k.

$U_{mn,t}$: indicates the status of tth spectrum slot at physical link (m, n), where $(m, n) \in L^s$, $t = 1, .., F$. It takes the value of 1 when tth frequency slot of link (m, n) is available, otherwise 0.

MD: an enumeration of modulation modes by their spectrum efficiencies. In this paper, we assume $MD = 1, 2, 3, 4, 6, 8$ for BPSK, QPSK, 8QAM, 16QAM, 64QAM, 256QAM, respectively.

d_{mn}: the length of physical link (m, n).

d_{mod}: the maximum transmission distance of the modulation mode mod, where $mod \in MD$.

R: a large integer.

Variables:

$M_{mn,a}^{ij}$: a Boolean variable. It takes the value of 1 when virtual link (i, j) is mapped to substrate network and traverses physical link (m, n) with the spectrum allocation starting from ath slot, otherwise 0.

A_k^i: a Boolean variable. It takes the value of 1 if virtual node i is mapped to physical node k, otherwise 0.

T_a^{ij}: a Boolean variable. It takes the value of 1 if virtual link (i, j) is mapped to substrate network with the spectrum allocation starting from ath slot, otherwise 0.

S^{ij}_{mod}: a Boolean variable. It takes the value of 1 if virtual link (i,j) chooses modulation mode mod, otherwise 0.

$Z^{ij}_{mn,a,mod}$: a Boolean variable. It equals to $M^{ij}_{mn,a}$ time S^{ij}_{mod}. It takes the value of 1 if virtual link (i,j) is mapped to substrate network and traverses physical link (m,n) with the spectrum allocation starting from ath slot ($M^{ij}_{mn,a} = 1$), and modulation mode mod is selected ($S^{ij}_{mod} = 1$), otherwise 0.

Objective:

$$\text{Min} \sum_{ij\in L^v}\sum_{mn\in L^s}\sum_{a=1,..,F}\sum_{mod\in MD} c_{mn}\Big(\Big\lceil\frac{p_{ij}}{mod}\Big\rceil + G\Big)Z^{ij}_{mn,a,mod} + \sum_{i\in N^v}\sum_{k\in N^s} c_k p_i A^i_k \tag{4}$$

The objective is to minimize the embedding cost in terms of spectrum slot cost and computation cost. The first term of Eq. (4) is the total spectrum slot cost. It is noted that one of the given modulation modes is selected for a virtual link embedding, and higher modulation mode selected, less spectrum slots are needed for the same value of bandwidth. The second term is the total computation cost. We allow that VN requests are blocked when the network resources are not enough where the ILP formulation gives infeasible solutions.

Constraints:

Virtual node embedding:

$$\sum_{k\in X(i)} A^i_k = 1; \qquad \forall i \in N^v \tag{5}$$

$$\sum_{i\in N^v} A^i_k \le 1; \qquad \forall k \in N^s \tag{6}$$

Equation (5) ensures that each virtual node is embedded to a physical node in the condition of geographical constraints, and Eq. (6) ensures that a physical node can host at most one virtual node of the VN request.

Virtual link embedding:

$$\sum_{a=1,..,F}\sum_{m\in N^s} M^{ij}_{mk,a} - \sum_{a=1,..,F}\sum_{n\in N^s} M^{ij}_{kn,a} = A^j_k - A^i_k; \quad \forall ij \in L^v, k \in N^s \tag{7}$$

Equation (7) derives the route of virtual link (i,j), where Eq. (7) has three forms according to the value of the right-hand side of the equation:

1) The right-hand side of Eq. (7) is equal to 0 (values of A^j_k and A^i_k are the same). According to Eq. (6), A^j_k and A^i_k can only be zero if they have the same value. Neither of end nodes of virtual link (i,j) is mapped to physical node k, then Eq. (7) ensures that for physical node k, the number of incoming physical links with spectrum allocations equals to the number of outgoing physical links with spectrum allocations;

2) The right-hand side of Eq. (7) is equal to 1 (A^j_k equals to 1 and A^i_k equals to 0). This means the end node j of virtual link (i,j) is mapped to physical node k, then at physical node k the number of incoming physical links with spectrum allocations is larger than the number of outgoing physical links with spectrum allocations by 1;

3) The right-hand side of Eq. (7) is equal to -1 (A^j_k equals to 0 and A^i_k equals to 1), means the source node i of virtual link (i,j) is mapped to physical node k. Accordingly, at physical node k, the number of outgoing physical links with spectrum allocations is larger than that of incoming physical links with spectrum allocations by 1.

Spectrum assignment:

$$\sum_{a=1,..,F} T^{ij}_a = 1; \qquad \forall ij \in L^v \tag{8}$$

$$\sum_{mn\in L^s} M^{ij}_{mn,a} \ge T^{ij}_a; \qquad \forall ij \in L^v, a = 1,..,F \tag{9}$$

$$\sum_{mn\in L^s} M^{ij}_{mn,a} \le R \cdot T^{ij}_a; \qquad \forall ij \in L^v, a = 1,..,F \tag{10}$$

Equation (8) ensures that only one spectrum allocation is secured to each virtual link mapping. Equations (9) and (10) ensure that T^{ij}_a has non-zero values only when virtual link (i,j) is mapped to physical link(s) with the spectrum allocation stating from ath slot.

Modulation mode selection:

$$\sum_{mod\in MD} S^{ij}_{mod} = 1; \qquad \forall ij \in L^v \tag{11}$$

$$\sum_{mn\in L^s}\sum_{a=1,..,F} M^{ij}_{mn,a} d_{mn} \le \sum_{mod\in MD} S^{ij}_{mod} d_{mod}; \quad \forall ij \in L^v \tag{12}$$

Equation (11) ensures that each virtual link is embedded to a physical path with a proper modulation mode. Equation (12) ensures that the signal transmission distance is within the range of the selected mode.

Network resources limitation:

$$\sum_{i\in N^v} p_i A^i_k \le U_k; \qquad \forall k \in N^s \tag{13}$$

$$\Big(\Big\lceil\frac{p_{ij}}{mod}\Big\rceil + G\Big)Z^{ij}_{mn,a,mod} \le \sum_{\substack{t=a,a+1,\\ ..,a+\lceil\frac{p_{ij}}{mod}\rceil+G-1}} U_{mn,t}; \quad \forall ij \in L^v, mn \in L^s, a = 1,..,F, mod \in MD \tag{14}$$

$$\sum_{ij\in L^v}\sum_{mod\in MD}\sum_{\substack{t=a-\lceil\frac{p_{ij}}{mod}\rceil-G+1,\\ a-\lceil\frac{p_{ij}}{mod}\rceil-G+2,..,a|t\ge 1}} Z^{ij}_{mn,t,mod} \le U_{mn,a}; \quad \forall mn \in L^s, a = 1,..,F \tag{15}$$

Equation (13) ensures that virtual nodes are only mapped to physical nodes with enough available computation resource.

Equation (14) ensures that enough spectrum slots are allocated for each virtual link mapping. Specifically, if a physical link (m,n) with the spectrum allocation starting from ath slot and modulation mode being mod is occupied by virtual link (i,j) with bandwidth requirement p_{ij}, then the spectrum slots

starting from a to $a+\lceil \frac{p_{ij}}{mod} \rceil + G - 1$ must be available for the allocation. This ensures the contiguity constraint of spectrum allocation.

Equation (15) ensures that a spectrum slot can be occupied by at most one virtual link. Specifically, at most one spectrum allocation containing the ath spectrum slot of physical link (m, n) is valid. For example, if virtual link (i, j) with bandwidth requirement p_{ij} is mapped to physical link (m, n) with modulation mode mod ($Z^{ij}_{mn,t,mod} = 1$), the spectrum allocations containing ath slot may range from $a - \lceil \frac{p_{ij}}{mod} \rceil - G + 1$ to a as the starting spectrum slot, so Eq. (15) ensures that at most one spectrum allocation takes ath slot if the slot is available.

Nonlinear equation conversion:

$$M^{ij}_{mn,a} + S^{ij}_{mod} - 1 \leq Z^{ij}_{mn,a,mod}; \quad \forall ij \in L^v, mn \in L^s, a = 1, .., F, mod \in MD \tag{16}$$

$$M^{ij}_{mn,a} + S^{ij}_{mod} \geq 2Z^{ij}_{mn,a,mod}; \quad \forall ij \in L^v, mn \in L^s, a = 1, .., F, mod \in MD \tag{17}$$

Equations (16) and (17) convert the nonlinear equation of $Z^{ij}_{mn,a,mod} = M^{ij}_{mn,a} \cdot S^{ij}_{mod}$ to linear equations.

A. ILP Problem Size

We calculate the numbers of variables and constraints to gain insights into the ILP problem. The number of variables is $O(|L^v||L^s||MD|F)$ and the number of constraints is $O(|L^v||L^s||MD|F)$. As network size grows, solving the ILP problem becomes prohibitively time-consuming.

B. A Six-node Example

An example of a six-node network that uses the ILP formulations to find an optimal solution is given below. The network topology is shown in Fig. 3, and the numbers next to links are fiber physical lengths in kilometers. It is noted that the set of physical nodes {0, 1, 2, 3} and the set of physical nodes {4, 5} are far from each other geographically, and only QPSK modulation mode is feasible. Ten randomly generated VN requests are given as the input in Table I. We used a commercial ILP solver, CPLEX [26], to solve the ILP problem formulated as described above, and the optimal embedding solutions are shown in Table I.

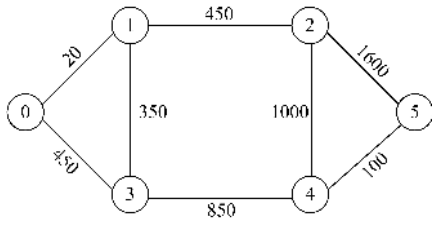

Fig. 3. A six-node network.

The arrivals and departures of ten VN requests are arranged with the simulated event sequence in the Table I. We see

TABLE I
OPTIMAL VNE SOLUTIONS OF TEN VN REQUESTS

No.	VN: $i \to j(p_i,p_j,p_{ij})$	$i : X(i)$	Solution: $m \to n[a,\text{slots},mod]$
VN1	(0→1)(3,1,7) (1→0)(1,3,2) (2→0)(2,3,5) (2→3)(2,1,3) (3→1)(1,1,4)	0:{4,5} 1:{4,5} 2:{0,1} 3:{2}	(4→5)[3,3,4] (5→4)[0,2,2] (1→3→4)[0,4,2] (1→2)[0,2,3] (2→4→5)[0,3,2]
VN2	(1→0)(3,1,2) (2→0)(4,1,9)	0:{0,1,3} 1:{4,5} 2:{0,1,3}	(4→3→1)[0,2,2] (0→1)[0,3,6]
VN2	Leave		
VN3	(0→1)(4,3,2) (1→0)(3,4,4) (2→1)(4,3,9) (3→0)(4,4,8)	0:{1,2} 1:{0,1,2,3} 2:{0,1,3} 3:{4,5}	(2→1)[0,2,2] (1→2)[2,3,2] (0→1)[0,3,6] (4→2)[0,5,2]
VN3	Leave		
VN4	(0→1)(4,4,1) (1→0)(4,4,3)	0:{0,1,2,3} 1:{4,5}	(3→4)[4,2,1] (4→3)[0,3,2]
VN5	(0→1)(1,1,7) (1→0)(1,1,2) (2→0)(3,1,9) (2→1)(3,1,5)	0:{4,5} 1:{1,3} 2:{4,5}	(4→3)[7,5,2] (3→4)[6,2,2] (5→4)[7,4,4] (5→4→3)[3,4,2]
VN6	(0→2)(3,3,2) (1→0)(3,3,6) (2→0)(3,3,7) (2→1)(3,3,3)	0:{0,1,2,3} 1:{0,1,3} 2:{0,1,2}	(1→0)[0,2,2] (3→1)[0,3,3] (0→1)[0,2,8] (0→1→3)[4,2,3]
VN6	Leave		
VN7	(1→0)(1,2,8) (2→0)(3,2,6) (3→2)(3,3,5)	0:{0,1,3} 1:{4,5} 2:{4,5} 3:{0,1,2}	(5→4→3→1)[12,5,2] (4→2→1)[0,4,2] (2→4)[3,4,2]
VN7	Leave		
VN8	(0→2)(2,3,7) (1→0)(1,2,7) (2→1)(3,1,1) (3→1)(3,1,4)	0:{0,1,3} 1:{0,1,2,3} 2:{4,5} 3:{4,5}	(1→3→4)[8,5,2] (3→1)[0,3,4] (4→3)[15,2,1] (5→4→3)[12,3,2]
VN1, 8	Leave		
VN9	(0→1)(3,4,7) (1→0)(4,3,5)	0:{0,1,2} 1:{0,1,2,3}	(1→0)[0,2,8] (0→1)[0,2,6]
VN4, 5, 9	Leave		
VN10	(1→0)(1,4,2)	0:{0,1,3} 1:{2}	(2→1)[0,2,2]
VN10	Leave		

that, in the condition of geographical constraints, some virtual nodes of a VN are embedded to a small geography range, and the virtual links are embedded to short physical paths. For example, virtual nodes 0 and 2 of VN2 are embedded to physical nodes 1 and 0, respectively, and virtual nodes 0, 1 and 2 of VN3 are embedded to physical nodes 2, 1 and 0, respectively, which forms small geography ranges in the graph. Then, high efficiency modulation modes can be used by physical paths to save spectrum resources, e.g. 256QAM are used by physical paths (0→1) in VN2 and VN3, where 3 and 3 spectrum slots with 256QAM are consumed comparing with the required 9 and 9 with BPSK, respectively. Meanwhile, if the geographical constraint makes virtual node embed to physical nodes that are far away from each other, short physical paths are also selected for the virtual links. For example, virtual nodes 0 and 3 of VN3 are embedded to physical nodes 2 and 4 under the geographical constraints, and the physical path (4→2) instead of other even longer paths, such as (5→2), is selected for a higher modulation application.

It is also noted that the optimal solutions prefer short length paths for virtual links with high bandwidth requirements. For example, the embeddings of VN2, VN3 and VN6 traverse physical link (0→1), which has the shortest fiber length and 256QAM can be applied to transmit between two nodes (VN2 and VN3 use 64QAM instead of 256QAM as they already use one spectrum slot for transmission, and one for guard band). Specifically, in these three requests, under the geographical constraints, the virtual links with high bandwidth requirements are embedded to the shortest physical link between node 0 and node 1 to maximize the modulation gain.

In the above example, it took tens of minutes for a PC with a 2.8 GHz CPU and 1024 MB RAM to solve the ILP problem based on the above described formulation. As this approach cannot scale to large networks, a scalable heuristic algorithm will be proposed. In the development of the heuristic algorithm, the following observations based on the above will be considered.

(1) The virtual node embedding of a VN should aim to reduce the distance range of the embedding physical nodes in the condition of geographical constraints.
(2) Virtual links with high bandwidth requirements should be embedded to short physical paths to increase the modulation gain in the condition of geographical constraints.

IV. Heuristic Algorithms

Motivated by the above observations, we propose three scalable heuristic algorithms for the VNE problem in flexi-grid networks. Instead of doing virtual node embedding and virtual link embedding in two steps, the proposed algorithms do them simultaneous, and embed a VN "link-by-link", where a "link" is a virtual link plus its two virtual end nodes.

In command line 1 of **Algorithm 1**, the current network is copied which is used for resource rollback if the VN request is finally blocked. In command line 2, a virtual link sorting algorithm, i.e. **Algorithm 2** or **3** or **4**, is called to set up the embedding order. The virtual links in front usually embed to shorter paths than the links at end. **Algorithm 2** sorts virtual links according to the degrees of their virtual end nodes. Command line 2 of **Algorithm 2** descendingly sorts virtual links according to the degree of their end node with the higher degree first, then in command line 3, among all virtual links that their higher degree end node have the same degree, the sorting is done descendingly according to the degree of their end node with the lower degree. Accordingly, virtual links connecting virtual nodes of high degrees are embedded first. **Algorithm 3** sorts virtual links according to the degree of their end node with the higher degree first (same as **Algorithm 2**), then among all virtual links that their higher degree end node have the same degree, the links are sorted according to the bandwidth requirements. This sequence makes the virtual links with end nodes of high degrees and high bandwidth requirements be embedded first. **Algorithm 4** sorts virtual links by bandwidth requirement, which makes the virtual links with high bandwidth requirements be embedded to short physical paths for high spectrum resource savings.

Algorithm 1: Virtual network embedding heuristics

Input: An arriving VN request $G^v(N^v, L^v)$, and current network $G^s(N^s, L^s)$.
Output: An embedding solution S in the current network, and updated network resources.
BEGIN:
1 $G \leftarrow G^s$.
2 Call **Algorithm 2** (or **Algorithm 3** or **Algorithm 4**) to set up virtual link embedding sequences and obtain a sorted virtual link set E.
//Embed each virtual link
3 **for** $e \in E$ **do**
4 **for** $md = |MD|$ *to 1* **do**
5 $g = \lceil \frac{p_{s(e)d(e)}}{md} \rceil + G$ ($s(e)$ and $d(e)$ are the source and the destination of e, respectively.)
6 **for** $a = 1$ *to* $F - g + 1$ **do**
7 Call **Algorithm 5** to build an auxiliary graph G^e with available spectrum slots from a to $a + g - 1$.
8 Find the shortest path P from $s(e)$ to $d(e)$ in G^e.
9 If a path cannot be found, Continue.
10 If $s(e)$ and $d(e)$ are embedded in a common physical node v in P, delete the higher cost dummy link of G^e between the two: one link from $s(e)$ to v and the other link from v to $d(e)$, go to Command line 7.
11 If P satisfies the distance constraint of modulation md, $S \leftarrow S + P$, Break.
  end
12 If a valid path is found, update the network resources of G, Break.
  end
13 If a path for e cannot be found, Return.
end
14 $G^s \leftarrow G$.
END

Algorithm 2: Sort virtual links by node degrees

Input: A VN $G^v(N^v, L^v)$.
Output: A sorted link set E.
BEGIN:
1 $E \leftarrow L^v$.
2 Sort E by the descending order of the degree of virtual end node with the higher degree of a link.
3 Among all virtual links that their higher degree of virtual end node have the same degree, sort these links in E by the descending order according to the degree of virtual end node with the lower degree.
END

Algorithm 3: Sort virtual links by node degrees and bandwidth requirements

Input: A VN $G^v(N^v, L^v)$.
Output: A sorted link set E.
BEGIN:
1 $E \leftarrow L^v$.
2 Sort E by the descending order of the degree of virtual end node with the higher degree of a link.
3 Among all virtual links that their higher degree of virtual end node have the same degree, sort these links in E by the descending order according to bandwidth requirements of virtual links.
END

Algorithm 4: Sort virtual links by bandwidth requirements

Input: A VN $G^v(N^v, L^v)$.
Output: A sorted link set E.
BEGIN:
1 $E \leftarrow L^v$.
2 Sort E by the descending order of bandwidth requirements of virtual links.
END

After the embedding sequence of virtual links is set up, each virtual link along with its end nodes is embedded following the sequence. In command line 4 of **Algorithm 1**, high modulations are tried before lower ones. The purpose is to reduce spectrum slot usages. In command line 7, an auxiliary graph with a modulation mode is built by **Algorithm 5** for a specific virtual link along with its two end nodes, and the virtual link embedding and the two virtual end node embeddings are converted to shortest path routing in the auxiliary graph. The auxiliary graph shown in Fig. 4(b) is for the virtual link (i, j) and two end nodes i and j, which is based on the substrate network in Fig. 4(a).

There are physical links (solid lines) and dummy links (dashed lines) in Fig. 4(b), where physical links are the links of the substrate network with sufficient available spectrum resources for the new connection and their lengths are within the transmission range of the given modulation (built by command line 3 of **Algorithm 5**), while a dummy link from

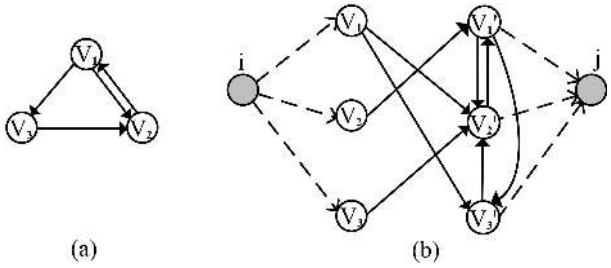

Fig. 4. (a) The substrate network. (b) The proposed auxiliary graph where the spectrum slots of the links from a_1 to a_2 are all available.

a virtual node to a physical node (or vice versa) indicates that the virtual node is hosted on the physical node (built by command lines 4 and 5 of **Algorithm 5**). In Fig. 4(b), to avoid virtual node i and j being mapped to a common physical node (constraint Eq. (6)), physical nodes are duplicated, and physical links are also duplicated as an original link from m to n becomes to be two new links from m to n' and from m' to n'.

The link cost of the auxiliary graph is set according to

$$c'_{mn} = \begin{cases} c_{mn} d_{mn} & m \neq i, n \neq j \\ R \cdot d'_{in} + r_{in}^{-1} & m = i \\ R \cdot d'_{mj} + r_{mj}^{-1} & n = j, \end{cases} \tag{18}$$

where the physical link cost is the weighted distance ($c_{mn} d_{mn}$), and the dummy link cost is the summation of the weighted average distance to physical nodes hosting virtual nodes ($R \cdot d'_{in}$ or $R \cdot d'_{mj}$) and the available resources (r_{in} or r_{mj}). It is noted that

$$d'_{in} = \frac{\sum_{v \ddot{\in} S} Dis(M_N(v), n)}{|\{v | v \ddot{\in} S\}|}$$

and

$$d'_{mj} = \frac{\sum_{v \ddot{\in} S} Dis(M_N(v), m)}{|\{v | v \ddot{\in} S\}|}$$

are the average distances of node n and node m to the physical nodes hosting virtual nodes, respectively, where $v \ddot{\in} S$ denotes the condition that node v hosts virtual nodes of the VN in solution S, and $Dis(M_N(v), n)$ is the distance between node $M_N(v)$ and node n. This strategy tries to limit the VNE solution within a small distance range, which is the first observation from the procedure in Table I. Because a virtual node is hosted on a physical node that may be a source or destination of multiple lightpaths in the substrate network, virtual node embedding is treated preferentially over virtual link embedding in our algorithm. To achieve this, the dummy link cost is deliberately multiplied by the large number R in Eq. (18), then the dummy link cost is significantly larger than the physical link cost, where shortest path algorithms prefer virtual node embedding first. The available resources

$$r_{in} = \frac{\sum_{e \in E(n)} \sum_{a=1,..,F} U_{s(e)d(e),a}}{|E(n)|} + \frac{\sum_{e \in Eo(n)} a_e}{|Eo(n)|}$$

and

$$r_{mj} = \frac{\sum_{e \in E(m)} \sum_{a=1,..,F} U_{s(e)d(e),a}}{|E(m)|} + \frac{\sum_{e \in Ei(m)} a_e}{|Ei(m)|}$$

denote the spectrum resources of physical links adjacent to node n and node m, respectively, where $E(n)$ is the set of adjacent links of node n, $Eo(n)$ is the set of adjacent outgoing links of node n, $Ei(m)$ is the set of adjacent incoming links of node m, and a_e is the number of spectrum allocations that p_{ij} requirement is accommodated by physical link e with the given modulation.

It is noted that, in our VNE heuristic algorithms, virtual links are embedded one-by-one following a sequence, and each virtual link along with its two end virtual nodes is embedded. However, a virtual node may have multiple incident virtual links, and the virtual node embedding in one virtual link embedding may affect the performance of other incident virtual link embeddings, this is because the sources or destinations of embedding lightpaths in the substrate network are already set. With the dummy link cost setting by Eq. (18), a virtual node is embedded to a physical node that: 1) has sufficient spectrum resources from physical links adjacent; 2) has a short average distance to the physical nodes that host virtual nodes of the request already. Then virtual links that have end nodes mapped already may find sufficient spectrum resources and short paths for embeddings, which increases the success probabilities of embeddings.

After the auxiliary graph is built in command line 7 of **Algorithm 1**, a shortest path algorithm is applied to derive the route in command line 8. If the derived path still has a common physical node embedding node i and j, the higher cost dummy link in the derived path is deleted from the auxiliary graph, and the heuristic algorithm runs again. Finally, the path length is checked to be within transmission ranges. If all virtual links are embedded successfully, the VN request is accommodated, otherwise the request is blocked.

The complexities of three virtual link sorting algorithms, **Algorithms 2**, **3** and **4**, are $O(|N^v||L^v|^2)$, $O(|N^v||L^v|^2)$ and $O(|L^v|^2))$, respectively. The building of an auxiliary graph by **Algorithm 5** has the complexity of $O(|L^s| + |N^v||N^s|)$ and the complexity of a shortest path algorithm is $O(|N^s|^2)$. In **Algorithm 1**, the inner operation of three loops (command lines 3, 4 and 6) has the complexity of $O(|N^s|^3)$ where the shortest path algorithm may be called $|N^s|$ times in the worst case.

We name three heuristic algorithms as **Heuristic-degree**, **Heuristic-degree&bandwidth**, and **Heuristic-bandwidth** when **Algorithm 2**, **Algorithm 3** and **Algorithm 4** are called in command line 1 of **Algorithm 1**, respectively. So, the three heuristic algorithms have the same complexity of $O(F|MD||L^v||N^s|^3)$.

Algorithm 5: Build an auxiliary graph

Input: A virtual link e, a spectrum band from slot a_1 to slot a_2, a modulation md and a partial embedding solution S.
Output: An auxiliary graph G^e.
BEGIN:

1 Add virtual nodes $s(e)$, $d(e)$ and all physical nodes into the empty graph G^e (each physical node n has a duplicated node n', called original physical node and duplicated physical node in G^e, respectively. Geographical constraint $X(i)$ is duplicated as $X'(i)$ accordingly, $i \in N^v$).
//Physical link constructions
2 **for** $l \in L^s$ **do**
3 If spectrum slots from a_1 to a_2 are available and the fiber length is within the maximal transmission range of the modulation md, add a link from $s(l)$ to $d(l)'$ and a link from $s(l)'$ to $d(l)'$ in G^e, then set link costs according to Eq. (18).
end
//Dummy link constructions
4 Check $s(e)$ in S. If $s(e)$ has been embedded already, connect $s(e)$ and the node in G^e, set the link cost to 0; otherwise, connect $s(e)$ to all original physical nodes in $X(i)$ that are with enough computation resources and have not embedded any virtual node of this VN yet, assign link costs according to Eq. (18).
5 Check $d(e)$ in S. If $d(e)$ has been embedded already, connect the node and $d(e)$ in G^e, set the link cost to 0; otherwise, connect all duplicated physical nodes in $X'(i)$ that are with enough computation resources and have not embedded any virtual node of this VN yet to $d(e)$, assign link costs according to Eq. (18).
END

V. Numerical Results

In this section, we present numerical results based on simulations to evaluate the performance of our proposed heuristic algorithms: Heuristic-degree, Heuristic-degree&bandwidth and Heuristic-bandwidth. As discussed above, for small sized problems, ILP can be used to allocate resources for each VN arrival. However, this does not mean that using ILP is optimal for a given order of arrivals because when we use ILP for a given arrival, we do not know the details of the future arrivals. Nevertheless, using ILP gives high quality solutions, and we use this approach as a benchmark for our heuristic algorithms. Accordingly, for the six-node network, we also provide benchmark simulation results obtained by an algorithm that uses ILP. Our performance measures include: blocking probability, average embedding cost, average modulation, average distance and average running time. Error bars of 95% confidence intervals based on Student's t-distribution are provided for all the simulation results. All the results presented and discussed in this section have been obtained using the above-mentioned PC with 2.8 GHz CPU and 1024 MB RAM.

The algorithms are evaluated in dynamic traffic scenarios, where VN request arrivals are assumed to follow a Poisson process with rate λ and their holding times are assumed to have a negative exponential distribution with a mean $1/\mu$. The traffic load of network is calculated as λ/μ (Erlang), and for simplicity, we set μ equal to 1 then the network load is λ (Erlang).

A. Numerical Results for the Six-node Network

The substrate network is shown in Fig. 3, and the computation capacity of a physical node is assumed to be 20 and the number of spectrum slots of a fiber link is set to 20 in this small network. VN requests are assumed to be connected directed graphs without loss of generality. The numbers of virtual nodes and virtual links of a VN request are uniformly distributed from 2 to 4 and from 1 to 5, respectively, and the computation and bandwidth requirements are uniformly distributed from 1 to 3 and from 1 to 9, respectively. The geographical constraints of virtual node embeddings are also generated in the substrate network with a random distance range among [400 km, 600 km]. We conduct 11 simulation experiments, each considering 50000 VN arrivals for the given demands.

Figures 5-9 present simulation results obtained in the six-node network shown in Fig. 3, where three heuristic algorithms and the ILP are compared. In Fig. 5, the blocking probabilities are compared which is calculated as the number of blocked VN requests to the total number of request arrivals. The blocking probabilities of four methods increase as network load increases. The ILP provides the lowest blocking probability, followed by Heuristic-bandwidth, Heuristic-degree&bandwidth and Heuristic-degree. The three heuristic algorithms have a similar blocking probability performance, and Heuristic-bandwidth performs the best. The reason is that the algorithm arranges the virtual links with high bandwidth requirements to be embedded first. This increases the possibility of finding a feasible path for the virtual link with a high bandwidth requirement and a short physical path is selected for less spectrum resource usage. Specifically, considering geographical constraints, there is a high possibility that a virtual link with a high bandwidth requirement has to use comparable long physical paths for embedding. If this virtual link is not embedded first, a longer path may have to be used, which may largely increase spectrum usages, or even a proper path cannot be founded. It is noted that with geographical constraints, the performance of VNE algorithms are related to the embeddings of the virtual links with high bandwidth requirements, because the spectrum usages or even request blockings may increase if longer paths are used. The other two algorithms embed virtual links with high virtual end node degrees first, which may lead the virtual links with high bandwidth requirements taking long paths or being blocked.

In Fig. 5, we observe larger confidence intervals for the lower range of network load when the blocking probability is small. This can be explained as follows: 1) lower network load results in rare blocking events for which it is more difficult to obtain accurate results with high confidence (short confidence intervals), and 2) the blocking probability values are on the log scale, which magnifies a small difference between two small values. Note that the confidence intervals can be in principle shortened by running longer simulations. However, there are limitations to the reduction of their lengths within realistic running times.

In Fig. 6, the average embedding cost of the accepted VN requests for the different algorithms are compared, where the average cost is calculated from the VNE costs of all accepted requests according to Eq. (4) averagely. All the values are unified based on the value of the ILP at network load of 0.8 Erlang. In particular the unified average embedding cost is the ratio of the average embedding cost to the average embedding cost of the ILP at network load of 0.8 Erlang. In the figure, the lowest value is the ILP, followed by Heuristic-bandwidth, Heuristic-degree&bandwidth and Heuristic-degree, and the Heuristic-bandwidth algorithm has about 10% higher cost than the ILP benchmark. The ILP not only obtains the lowest blocking probability, but also the lowest average embedding cost, which is at the cost of intensive computations and cannot scale. The same reason mentioned in Fig. 5 can also explain why Heuristic-bandwidth has lower cost values than Heuristic-degree&bandwidth and Heuristic-degree, which is that the algorithm embeds the virtual links with high bandwidth requirements first, and short physical paths with small spectrum usages are applied.

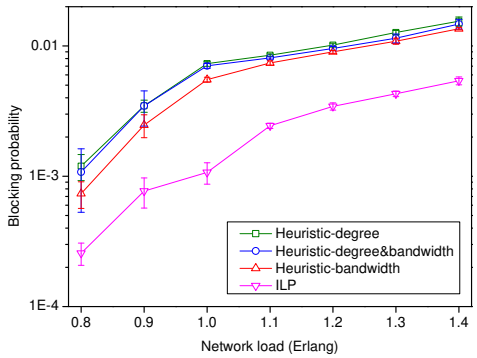

Fig. 5. Comparison of blocking probability in the six-node network.

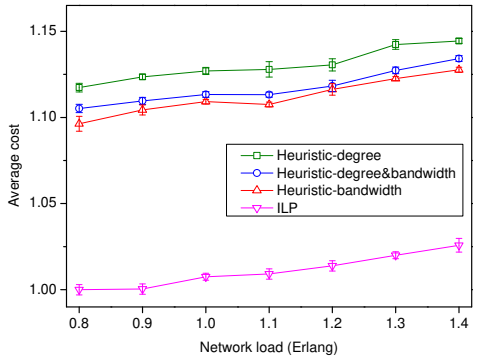

Fig. 6. Comparison of average embedding cost in the six-node network.

Figures 7 and 8 provide comparisons of the average modulation and average distance of virtual links among the algorithms, respectively. The average modulation is the modulations used by virtual links of all accepted VN requests averagely, and the average distance (km) is the physical path lengths of virtual link embeddings averagely. In Fig. 7, the three heuristic algorithms have similar average modulations and are higher than the ILP. Meanwhile, the three heuristic algorithms have longer average distance paths than the ILP shown in Fig. 8. This is because, with geographical constraints, the three heuristic algorithms can not derive the optimal paths

as the ILP does, then long paths are used. In the algorithms, we try to use high-order modulation format to reduce the spectrum slot usage, which is shown as Eq. (3). However, because of the granularity of optical communication, there are cases where both a high-order modulation format and a low-order modulation format lead to the same spectrum usage. For example, in Table I, VN6 has a virtual link (0→2) being embedded to physical link (1→0), QPSK and one spectrum slot are used to provide 2 units transmission rate. In this case, other higher-order modulation formats, like 8QAM, 16QAM also have sufficient transmission distance to cover the physical link (1→0), and the same number of spectrum slots is used, i.e. $\lceil \frac{2}{2} \rceil = \lceil \frac{2}{3} \rceil = \lceil \frac{2}{4} \rceil = 1$. For this case, a lower order modulation (QPSK) is chosen for better signal quality at the receiver by the ILP, but the three heuristic algorithms try to use high modulations to reduce the spectrum usage, so the ILP results in a shorter average distance and a lower average modulation usage than the three heuristic algorithms.

It is also noted that in Fig. 8, Heuristic-degree has smaller values than Heuristic-degree&bandwidth and Heuristic-bandwidth. This is because Heuristic-degree embeds the virtual links with high virtual end node degrees first to reduce physical path lengths of multiple virtual links simultaneously, which may lead to a shorter average distance, but to longer physical paths for the virtual links with high bandwidth requirements.

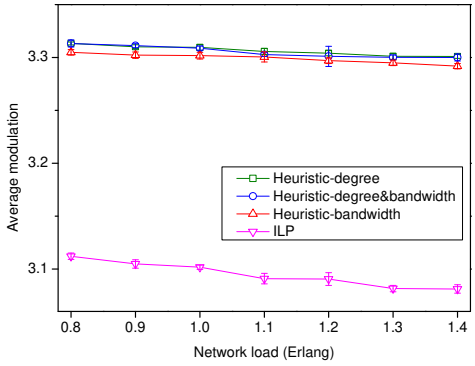

Fig. 7. Comparison of average modulation mode used by virtual links in the six-node network.

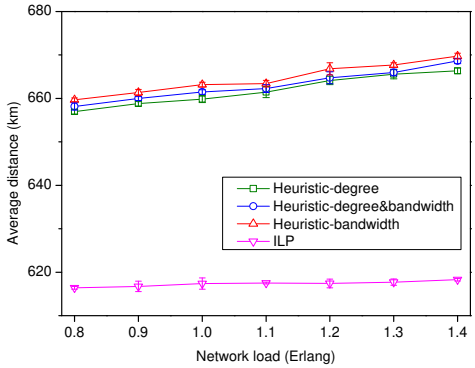

Fig. 8. Comparison of average distance of virtual links embedded in the six-node network.

The average running times are shown in Fig. 9, which is the time used to process a VN request averagely. The three heuristic algorithms have similar running time, because of the same algorithm complexity. The running time of the heuristic algorithms is two orders of magnitude shorter than that of the ILP.

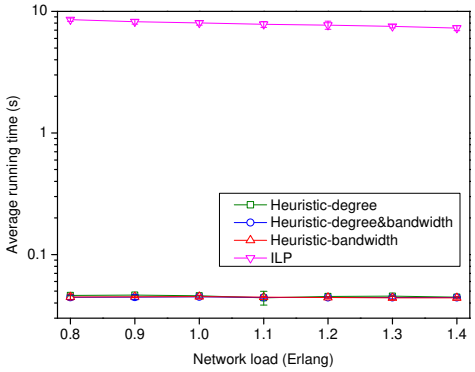

Fig. 9. Comparison of average running time for VN requests in the six-node network.

B. Numerical Results for 100-node random Networks

Because ILP is not scalable, in this subsection, we compare the performance of the three heuristic algorithms in 100-node random substrate networks, where the average node degree is 2.5, the computation capacity of a physical node is assumed to be 100 and the number of spectrum slots of a fiber link is set to 100, the lengths of fiber links are randomly generated in [10 km, 900 km]. The numbers of virtual nodes and virtual links of a VN request are uniformly distributed from 2 to 6 and from 1 to 10, respectively, and the computation and bandwidth requirements are uniformly distributed from 5 to 15 and from 5 to 50, respectively. The geographical constraints of virtual node embeddings are also generated in the substrate network with a random distance range among [700 km, 1300 km]. We conduct 21 simulation experiments, each involving 500,000 VN arrivals, and show the average values with a confidence interval of 95%.

Figures 10-14 present simulation results obtained in 100-node random networks. The same measurements as in the six-node network are compared among the three heuristic algorithms. In Fig. 10, Heuristic-bandwidth is shown to achieve the lowest blocking probability, followed by Heuristic-degree&bandwidth and Heuristic-degree. For the results presented in Fig. 11, the unified average embedding cost is the ratio of the average embedding cost to the average embedding cost of the Heuristic-bandwidth algorithm at network load of 0.5 Erlang. In the figure, Heuristic-bandwidth has the lowest value, followed by Heuristic-degree&bandwidth and Heuristic-degree, which is the same order observed in the blocking probability comparison in Fig. 10. This is because a lower average embedding cost implies lower network resource usage by requests, then more requests can be accommodated by limited network resources, leading to a lower blocking probability.

Figures 12 and 13 show the average modulation and the average distance of virtual links, respectively. In

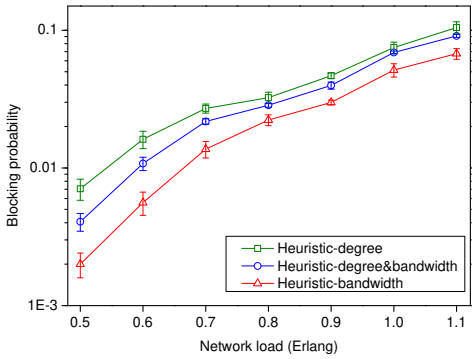

Fig. 10. Comparison of blocking probability in 100-node networks.

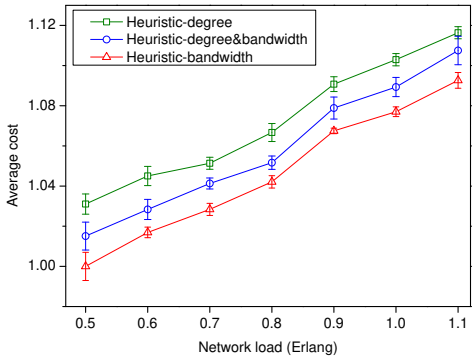

Fig. 11. Comparison of average embedding cost in 100-node networks.

Fig. 12, Heuristic-degree has the highest average modulations, followed by Heuristic-degree&bandwidth and Heuristic-bandwidth averagely. Meanwhile, in Fig. 13, Heuristic-degree has the shortest average distance values, followed by Heuristic-degree&bandwidth and Heuristic-bandwidth. This verifies that short paths can use high modulations. Although Heuristic-bandwidth uses the longest path for VN request, it can find shorter path and use less network resources for the virtual links with high bandwidth requirements, which is the main factor deciding the algorithm performance. When network load increases, the average modulation of the three algorithms decreases and the average distance increases, because longer paths are used for virtual link embedding to accommodate more requests with limited network resources. It is noted that when the network load is 0.5 Erlang, there are sufficient network resources to accommodate a VN request. All three heuristic algorithms can find sufficiently short physical paths of similar length for virtual link embeddings. In this case, the three algorithms have close average distance values in Fig. 13. For the same reason, the average modulation results for the case of 0.5 Erlang load in Fig. 12 are also close to each other.

In Fig. 13, the average distances significantly increase with the increase of the network load comparing to the little sensitivity of average distance against network load in the six-node network as shown in Fig. 8, where for ILP, the average distance is close to 620 km, and for the heuristic algorithm it hovers around 660 km. This different behavior can be explained by the fact that small networks provide a small number of possible physical paths required for virtual link embeddings. When network load increases, in the 100-node network, there is a much higher possibility to find an alternative feasible physical path than in the six-node network because of more potential physical paths between two nodes. Therefore, as the network load increases, in the 100-node network, we are forced to choose longer and longer paths which increase the average distance. This effect does not appear in the six-node network because of the limitation of alternative paths.

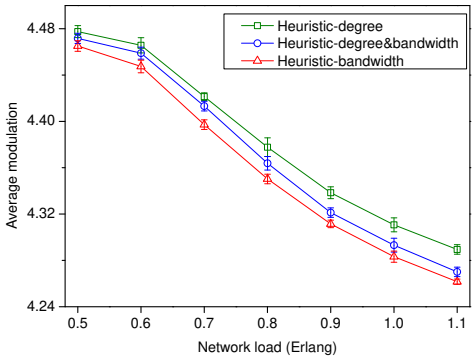

Fig. 12. Comparison of average modulation mode used by virtual links in 100-node networks.

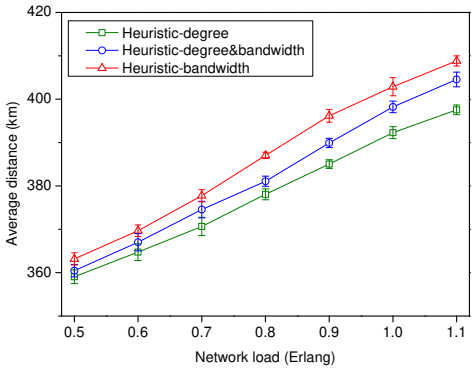

Fig. 13. Comparison of average distance of virtual links in 100-node networks.

Figure 14 provides the average running time of VNEs for a large network. Due to the same complexity, the three algorithms have very close running times.

VI. Conclusion

We have considered the VNE problem with dynamic traffic in flexi-grid networks where different modulation modes are used in optical channels to reduce spectrum usages. We have proposed an ILP formulation and three heuristic algorithms based on insights from the former, namely, Heuristic-degree, Heuristic-bandwidth and Heuristic-degree&bandwidth. The numerical results reveal that: 1) the three heuristic algorithms have similar blocking probabilities and the Heuristic-bandwidth algorithm achieves the lowest value among three algorithms. This is because, under geographical constraints, the Heuristic-bandwidth algorithm aims to not only embed the virtual links with high bandwidth requirements to obtain a large modulation gain, but also improve the success probability

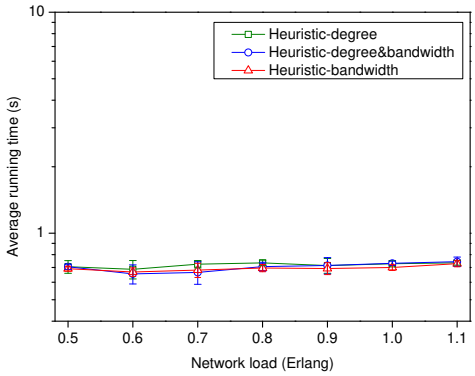

Fig. 14. Comparison of average running time for VN requests in 100-node networks.

of these virtual link embeddings; 2) the blocking probabilities obtained by the Heuristic-bandwidth algorithm are slightly closer to that of the ILP benchmark than the other two heuristic algorithms, and the Heuristic-bandwidth algorithm requires about 10% higher average embedding cost than the ILP benchmark. However, since the ILP is not scalable for realistic size networks, somewhat less efficient heuristic algorithms are required; 3) the Heuristic-bandwidth algorithm trades the accuracy with time-efficiency, where the the running time of the algorithm for each VN request is two orders of magnitude shorter than that of the ILP in the six-node network.

REFERENCES

[1] Cisco Inc., "White paper: Cisco VNI forecast and methodology, 2015–2020," 2015.

[2] B. Han, V. Gopalakrishnan, L. Ji, and S. Lee, "Network function virtualization: Challenges and opportunities for innovations," *IEEE Commun. Mag.*, vol. 53, no. 2, pp. 90–97, 2015.

[3] R. Mijumbi, J. Serrat, J. L. Gorricho, N. Bouten, F. D. Turck, and R. Boutaba, "Network function virtualization: State-of-the-art and research challenges," *IEEE Commun. Surv. Tutorials*, vol. 18, no. 1, pp. 236–262, 2016.

[4] N. Feamster, L. Gao, and J. Rexford, "How to lease the internet in your spare time," *SIGCOMM Comput. Commun. Rev.*, vol. 37, no. 1, pp. 61–64, 2007.

[5] A. Fischer, J. Botero, M. Beck, H. De Meer, and X. Hesselbach, "Virtual network embedding: a survey," *IEEE Commun. Surv. Tutorials*, vol. 15, no. 4, pp. 1888–1906, 2013.

[6] O. Gerstel, M. Jinno, A. Lord, and S. J. B. Yoo, "Elastic optical networking: a new dawn for the optical layer?" *IEEE Commun. Mag.*, vol. 50, no. 2, pp. s12–s20, 2012.

[7] E. Palkopoulou, G. Bosco, A. Carena, D. Klonidis, P. Poggiolini, and I. Tomkos, "Nyquist-WDM-based flexible optical networks: Exploring physical layer design parameters," *J. Lightwave Technol.*, vol. 31, no. 14, pp. 2332–2339, 2013.

[8] D. Hillerkuss et al., "Single-laser 32.5 Tbit/s Nyquist WDM transmission," *IEEE/OSA J. Opt. Commun. Netw.*, vol. 4, no. 10, pp. 715–723, 2012.

[9] G. Shen and M. Zukerman, "Spectrum-efficient and agile CO-OFDM optical transport networks: architecture, design, and operation," *IEEE Commun. Mag.*, vol. 50, no. 5, pp. 82–89, 2012.

[10] G. Zhang, M. D. Leenheer, A. Morea, and B. Mukherjee, "A survey on OFDM-based elastic core optical networking," *IEEE Commun. Surv. Tutorials*, vol. 15, no. 1, pp. 65–87, 2013.

[11] J. Lu and J. Turner, "Efficient mapping of virtual networks onto a shared substrate," *Technical Report WUCSE-2006-35, Washington University*, 2006.

[12] I. Houidi, W. Louati, and D. Zeghlache, "A distributed virtual network mapping algorithm," in *Proc. ICC*, 2008, pp. 5634–5640.

[13] A. Jarray and A. Karmouch, "Decomposition approaches for virtual network embedding with one-shot node and link mapping," *IEEE/ACM Trans. Netw.*, vol. 23, pp. 1012–1025, 2015.

[14] M. Yu, Y. Yi, J. Rexford, and M. Chiang, "Rethinking virtual network embedding substrate support for path splitting and migration," *SIGCOMM Comput. Commun. Rev.*, vol. 38, no. 2, pp. 17–29, 2008.

[15] J. Lischka and H. Karl, "A virtual network mapping algorithm based on subgraph isomorphism detection," in *Proc. SIGCOMM Workshop on Virtualized Infrastruct Systems & Architectures*, 2009, pp. 81–88.

[16] M. Chowdhury, M. R. Rahman, and R. Boutaba, "Vineyard: Virtual network embedding algorithms with coordinated node and link mapping," *IEEE/ACM Trans. Netw.*, vol. 20, no. 1, pp. 206–219, 2012.

[17] L. Gong, W. Zhao, Y. Wen, and Z. Zhu, "Dynamic transparent virtual network embedding over elastic optical infrastructures," in *Proc. ICC*, 2013, pp. 3466–3470.

[18] L. Gong and Z. Zhu, "Virtual optical network embedding (VONE) over elastic optical networks," *J. Lightwave Technol.*, vol. 32, no. 3, pp. 450–460, 2014.

[19] M. Jinno, B. Kozicki, H. Takara, A. Watanabe, Y. Sone, T. Tanaka, and A. Hirano, "Distance-adaptive spectrum resource allocation in spectrum-sliced elastic optical path network," *IEEE Commun. Mag.*, vol. 48, no. 8, pp. 138–145, 2010.

[20] K. Christodoulopoulos, I. Tomkos, and E. Varvarigos, "Elastic bandwidth allocation in flexible OFDM-based optical networks," *J. Lightwave Technol.*, vol. 29, no. 9, pp. 1354–1366, 2011.

[21] C. Wang, G. Shen, and S. K. Bose, "Distance adaptive dynamic routing and spectrum allocation in elastic optical networks with shared backup path protection," *J. Lightwave Technol.*, vol. 33, no. 14, pp. 2955–2964, 2015.

[22] A. Cai, J. Guo, R. Lin, G. Shen, and M. Zukerman, "Multicast routing and distance-adaptive spectrum allocation in elastic optical networks with shared protection," *J. Lightwave Technol.*, vol. 34, no. 17, pp. 4076–4088, 2016.

[23] A. Bocoi, M. Schuster, F. Rambach, M. Kiese, C. A. Bunge, and B. Spinnler, "Reach-dependent capacity in optical networks enabled by OFDM," in *Proc. OFC*, 2009, pp. 1–3.

[24] B. C. Chatterjee, N. Sarma, and E. Oki, "Routing and spectrum allocation in elastic optical networks: A tutorial," *IEEE Commun. Surv. Tutorials*, vol. 17, no. 3, pp. 1776–1800, 2015.

[25] M. Klinkowski, M. Ruiz, L. Velasco, D. Careglio, V. Lopez, and J. Comellas, "Elastic spectrum allocation for time-varying traffic in flexgrid optical networks," *IEEE J. Sel. Areas Commun.*, vol. 31, no. 1, pp. 26–38, 2013.

[26] ILOG CPLEX, ILOG, Inc., Mountain View, CA[Online], Available: http://www.ilog.com/products/cplex/.